Mineralogy and texture of the Storforshei iron formation, and their effect on grindability

Marte Kristine Tøgersen[1,2], Rolf Arne Kleiv[1], Steinar Ellefmo[1] and Kurt Aasly[1]

[1]*Department of Geoscience and Petroleum, Norwegian University of Science and Technology, Sem Sælandsveg 1, N-7491 Trondheim, Norway*

[2]*Rana Gruber AS, Mjølanveien 29, Gullsmedvik, 8601 Mo i Rana, Norway*

Abstract

Investigating how ore mineralogy and texture affect the recovery from the processing plant is important for any mining operation. The results will assist in production planning and optimising the utilisation of a deposit. Easily available validated tests are desirable and useful.

The Storforshei iron formation (IF) consists of several iron oxide deposits with mineralogical and textural differences. Although the Fe grades of the ores are similar, mineralogical and textural characteristics of the deposits affect the individual recoveries from the magnetic separation. For this paper three of the ore deposits were sampled, and important mineralogical and textural properties were investigated and tested. The investigations included geological mapping and optical microscopy, and the test work involved surface hardness measurements by Schmidt hammer and Equotip, and autogenous milling tests (i.e., grindability). The aim of the study was to investigate whether ore mineralogy and textures can be correlated to surface hardness measurements, and whether these three parameters can be used to evaluate grindability. The ores were classified into six ore types based on mineralogy and textures. The results show that the ore mineralogy and texture influence the surface hardness. Fine-grained ore types with irregular-to-no visible grain boundaries have higher surface hardness than coarser-grained ore types with straight grain boundaries. Furthermore, surface hardness measurements and grindability evaluations (using throughput (kg/h) and specific energy consumption (kWh/tonne)) of samples from three of the iron oxide deposits indicate that grindability decreases with increasing surface hardness. The relationship found between the parameters ore mineralogy, texture, surface hardness, and grindability suggests that geological mapping and surface hardness measurements can be used to evaluate grindability, and thus assess ore processing performance.

Keywords: Storforshei iron formation, surface hardness, texture, ore mineralogy, grindability

1 Introduction

Rana Gruber AS (RG AS) currently mines iron ore from underground and open pit operations in the Dunderlandsdalen valley, about 30 km north east of Mo i Rana, Nordland County, Norway. Four million tonnes of iron ore are mined from the Kvannevann deposit annually, and the main products are hematite and magnetite concentrates. There are 13 ore deposits in the Storforshei IF, with varying mineralogical and textural properties leading to variable recovery. The mineral processing at RG AS includes autogenous (AG) milling, wet low-intensity magnetic separation (LIMS) followed by wet high-intensity magnetic separation (WHIMS). The AG mills are in closed circuit, with 800 µm screens. The d_{80} of the mill circuit product is 210 µm.

The Kvannevann- and Stortjønna iron ores have a total Fe content of 34 wt % (NGU, 2017). The Stortjønna open pit was abandoned in 2013 after 2 years in production because recoveries did not reach expected levels, indicating that other properties than grade affect recovery. Samples were collected from the Kvannevann and Stortjønna deposits. Additionally, the Stensundtjern deposit, a possible upcoming mining target in the Storforshei IF, was included in this study.

The aim of the research presented in this paper was to investigate the effect of ore mineralogy, texture, and surface hardness on the ore grindability and on the particle size distribution of the mill circuit products. The throughput (kg/h) and specific energy consumption (kWh/tonne) in the AG mill were used to determine grindability.

The classification of ore types is based on mineralogical and textural characteristics of the iron ores. Contrary to previous work (e.g., Lopera, 2014; Mwanga et al., 2015), the classification is performed before surface hardness measurements and grindability testing. This approach is similar to the work of Voordouw et al. (2010) where platinum mineral assemblages were grouped based on ore mineralogy and trace elements. Lund (2013) defined preliminary geometallurgical ore types first according to mineralogy and geochemistry, and later included ore texture. Others like Lopera (2014) and Niiranen (2015) used surface hardness and mill tests to divide ores into different comminution domains.

The main objective of the present study was to provide increased predictability in the processing of highly metamorphosed iron ores. If surface hardness can be used to evaluate grindability, the iron ores can be tested by easy, fast and non-destructive methods prior to mineral processing.

The main research questions were:

- Is it possible to correlate ore mineralogy and texture with surface hardness?
- How is grindability affected by ore mineralogy and textures?
- Can surface hardness be used to evaluate grindability?

2 Background

2.1 Geological setting

The Storforshei IF is a metasedimentary iron formation and part of the Dunderland formation, located in the Uppermost Allochthon in the Norwegian Caledonides (Søvegjarto, 1972; Grenne et al., 1999). The IF belongs to a series of iron formations located between the city of Mosjøen (lat. 65°20') in the south to the city of Tromsø in the north (lat. 69°40'), a distance of 550 km (Melezhik et al., 2015). The Storforshei IF is the only iron formation currently mined in Norway, and the main economic minerals according to NGU (2017) are hematite (40 %) and magnetite (5 %). The Neoproterozoic host rocks are mainly marbles and mica schists (Bugge, 1948; Søvegjarto, 1972). The sedimentary precursor of the IF was deposited on a carbonate-silica-rich shelf which was located either near a microcontinent or on the margin of Laurentia (e.g., Grenne et al., 1999; Melezhik et al., 2015). After deposition, the iron formation was subjected to several deformation phases, dominated by the Caledonian orogeny where Laurentia and Baltica collided (Søvegjarto, 1972; Roberts and Gee, 1985). The Storforshei IF was subjected to amphibolite facies metamorphism and is intensely banded reflecting mineralogy and textures (Søvegjarto, 1972; Ellefmo, 2005). The geology of the relevant area is shown in Figure 1. The locations of the sampled deposits; Kvannevann, Stortjønna and Stensundtjern are highlighted on the map. Stensundtjern is a separate ore horizon located to the west in the Dunderlandsdalen valley. Kvannevann and Stortjønna belong to the same ore horizon. Kvannevann is larger than Stensundtjern, while Stortjønna is notably smaller than the other two deposits.

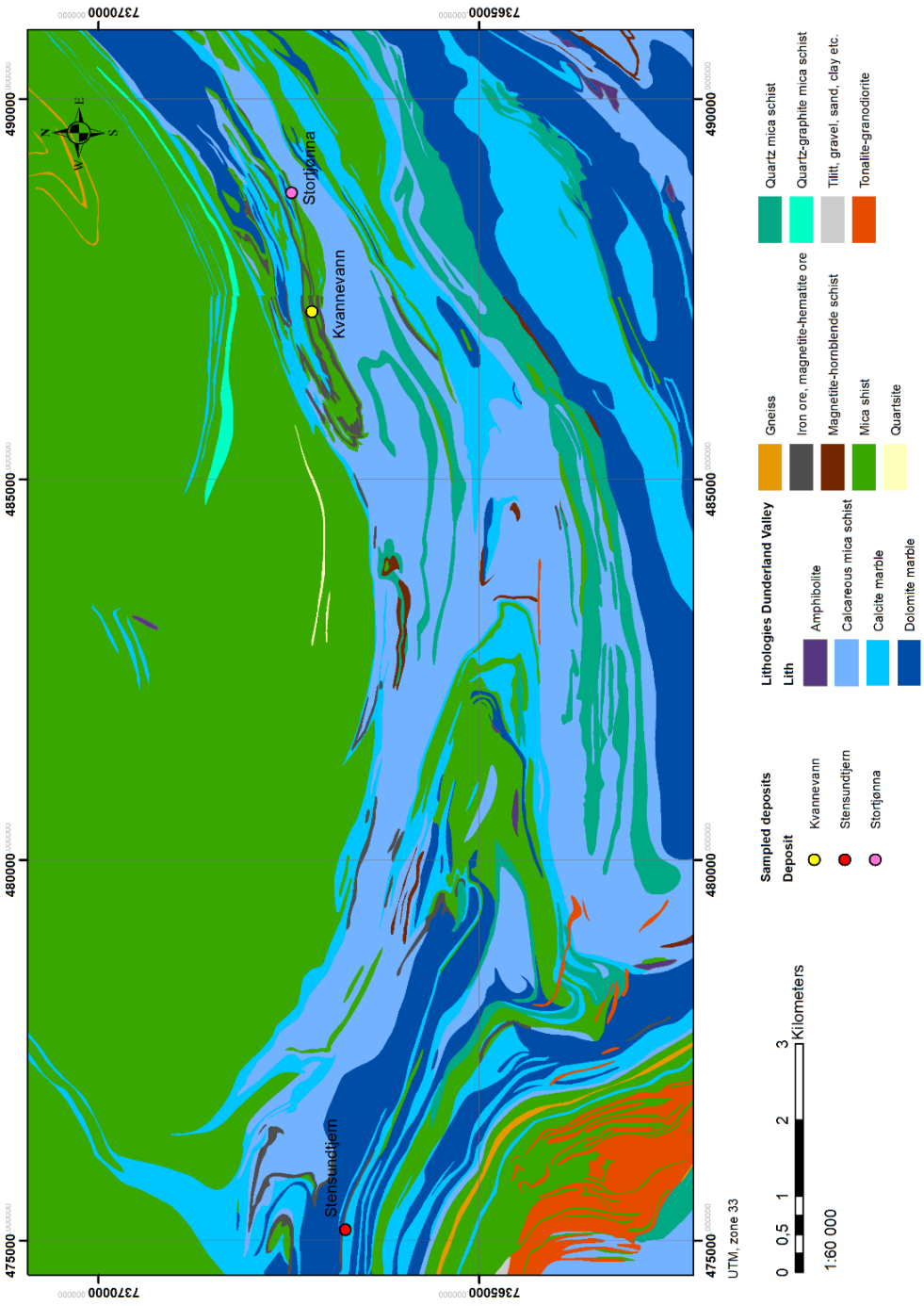

Figure 1: Geology of the Storforshei area, showing the location of the magnetite-hematite iron ores in Storforshei iron formation. The geology is compiled from Søvegjarto et al. (1989) and Gjelle et al. (1991).

2.2 Previous relevant geometallurgical research

Lund (2013) quantified mineral processing properties of apatite-magnetite ores and developed a geometallurgical program for the Malmberget iron ore (Sweden), which enabled improved production and resource utilisation (Lund, 2013) based on a comprehensive characterisation and analyses of the

iron ores. However, no surface hardness measurements or grindability tests were reported. Niiranen (2015) performed comminution tests on three apatite-magnetite ore types from the Kiirunavaara iron ore. The ore types were defined by their SiO_2 and P contents. After comminution, one ore type was divided into two subgroups, and a link between mineralogy and grindability was established. Available literature (i.e., Lund, 2013; Niiranen, 2015) focuses mainly on high-grade magnetite dominant ores; hence the present study contributes to increased knowledge on the processing behaviour of low-grade hematite ores.

The Schmidt hammer method is widely used in concrete and rock characterisation (e.g., Deere and Miller, 1966 and Szilágyi et al., 2009). Viles et al. (2011) used the Schmidt hammer and Equotip methods on dimension stone and demonstrated difficulties in comparing the two methods. Mining related research has focused on developing simple procedures to categorise ore types to predict comminution behaviour (e.g., Hunt, 2013; Lopera, 2014). Rock mechanical tests such as the JK Tech drop weight test (Napier-Munn et al., 1996), the JK Rotary Breakage Test (Shi et al., 2009), the SMC test (Morrell, 2004), and standard Bond grindability test (Bond, 1952) require at least 10 kg of material. The amount of material required for the procedures may, according to Mwanga et al. (2015), be an issue for greenfield exploration activities. Hence, Mwanga et al. (2015) developed the geometallurgical comminution test (GCT) as an approach to achieve representative results for test batches of 220 g material. The GCT is a small-scale comminution test which makes use of a lab-scale jaw crusher, a screen, and a small laboratory tumbling mill. Mwanga et al. (2015) argued that the GCT is a cost and time-efficient test that provides substantial data from limited sample sizes.

Ores are additive if the grindability of an ore blend is the same as the weighted average grindability of the ore types in the blend (e.g., Van Tonder et al. 2010 and the references therein). To evaluate grindability of an ore with notable internal variability in mineralogy and texture, larger homogenised test batches are needed to get representative and reliable results. Van Tonder et al. (2010) investigated mineral processing of platinum ores and the effect of ore blending in Rustenburg, South Africa. The ore blend consisted of four rather homogenous different ore types with a high inter-ore-type variability. They found through lab-scale tests that blends of ore types with varying metallurgical properties displayed non-additive characteristics. Larger test batches will therefore improve the prediction capabilities of the production-scale non-additive grindability.

Understanding the effect of mineralogy, geochemistry, lithology, and alteration on the comminution processes are valuable for processing any ore. Hunt et al. (2013) successfully modelled comminution parameters using information obtained from drill core logs, together with measured comminution data collected on site. The drill core log information included lithology and alteration type, as well as mineralogy and chemistry data. Hunt (2013) included Semi-Autogenous Grinding Power Index (SPI), Bond Work Index (BWI), and Julius Kruttschnitt Mineral Research Centre (JKMRC) drop weight test

(A*b) as parameters to characterise the comminution behaviour. These indices and tests were selected because they can be conducted at low cost and on drill core samples. Hunt et al. (2013) stressed the need to classify sample sets based on alteration type and lithology to identify correlations between mineralogy or chemistry and grindability. Lopera (2014) used surface hardness data together with mineralogy, chemistry, and a range of comminution tests to define comminution domains. Surface hardness measurements were collected from drill cores and hand specimens representing different lithologies. Surface hardness values varied between lithologies and were low in tectonically-induced weakness zones. Within each lithology variability was low (Lopera, 2014). Kekec et al. (2006) investigated the effect of rock textures on comminution. The investigations were based on experiments on different types of rock (granite, marble, travertine, and andesite). They observed that rocks of similar origin show differences in the crushing and grindability behaviour caused by the differences in rock texture. Xu et al. (2013) found that the specific energy required for breakage of a copper ore increases with decreasing particle size, and that grain boundary fractures require relatively low specific energy. By characterising the geochemistry, mineralogy, and grindability of the cemented layer, Philander and Rozendaal (2011) improved the mill design to accommodate a complex calcium-magnesium-rich cemented layer, part of the clastic Cainozoic ore-bearing sequence in the Namakwa Sands heavy mineral deposit (Brand-se-Baai, South Africa), previously not viable for production.

3 Materials and methods

3.1 Materials

The Kvannevann-, Stortjønna-, and Stensundtjern iron ore deposits found in the Storforshei IF were sampled for pilot scale testing. One truck-load (40 tonnes) from blasts in the geographical centre (Figure 1) of each deposit was crushed with a mobile jaw crusher. The sampling point was at the end of the associated conveyor belt. The entire width of the material stream was collected into a big bag. Representative samples from the conveyer belt were obtained by collecting several increments at regular intervals during crushing (3x10 s per big bag). A total of 2 tonnes, in two big bags, were sampled from the conveyer belt for each deposit. D_{50} of the Kvannevann, Stensundtjern, and Stortjønna crusher products were 70 mm, 38 mm, and 100 mm, respectively, while the top size was 300 mm in all three products. In the lab, one sub-sample for particle size distribution analysis was split from each 2-tonne sample by quartering. Hand specimens (5-10 kg) displaying mineralogical and textural variations were sampled from the three deposits. Polished thin sections were made from 20 of the selected hand specimens, at the Department of Geoscience and Petroleum. Also, split drill cores (42 mm diameter) were made available by RG AS for surface hardness tests.

3.2 Methods

3.2.1 Microscopy

A Nikon Eclipse E600 petrographic light microscope with Diagnostic Instruments Inc. Spot IN320 colour digital camera was used to document and identify mineralogy and textures. A Hitachi SU-6600 low vacuum field emission scanning electron microscope (SEM) with two Bruker XFlash 5010 energy-dispersive X-ray spectroscopy (EDS) detectors, was used for collecting x-ray analyses of minerals, with a 30s counting time per point. The SEM was run at 20 kV and 0.49 nA beam current.

3.2.2 Surface hardness measurements

A *Proseq Type L Original Schmidt hammer* (Schmidt hammer) was used to measure surface hardness of boulders, and a *Proseq Type D Equotip 3* (Equotip) instrument was used on drill cores. Both instruments measure the rebound energy after delivering a given impact energy to the sample. The Schmidt hammer has an impact energy of 0.735 N m and measuring range from 10-70 N/mm^2 compressive hardness (Proseq.com, 2016). The Equotip instrument delivers an impact energy of 11 N mm to the samples, and it can measure a maximum sample hardness of 890 HLD. The Leeb Hardness (HL) is calculated from the rebound velocity v_r and the impact velocity v_i ratio. The "D" in HLD reflects the type of Equotip used (Proseq.com, 2016).

The Schmidt hammer measurements were conducted on non-weathered surfaces of roughly 0.5 m^3 boulders obtained from blasts. Twenty measurements were conducted both parallel and perpendicular to the foliation. For boulders with no foliation, 20 measurements were collected from only one surface. Following the standard of the International Society for Rock Mechanics (1978), the 10 lowest values were discarded from each dataset of 20 measurements.

The selection of drill cores for Equotip measurement was based on the drill core logs and their locations in the iron formation. Based on procedures defined by Lopera (2014) and local lithological variations, measurements were taken every 3 cm along the core. All measurements under 100 HLD were discarded (only 5 out of 5689 measurements). The low HLD values are assumed to be incorrect measurements because of temporarily inaccuracies in the execution of the measuring procedures.

A total of 5689 points on drill cores were measured using the Equotip, while 34 boulders were measured using the Schmidt hammer. All ore types were measured by the Equotip, while all but the ore types Hematite-Magnetite and Magnetite-Ore (section 4.1) were measured by Schmidt hammer. The reason for not measuring these two ore types with Schmidt hammer was lack of suitable specimens.

3.2.3 Pilot-scale autogenous (AG) milling

Wet closed-circuit pilot-scale milling of the Kvannevann, Stensundtjern, and Stortjønna samples were performed using an AG mill (inner dimensions: Ø 0.69 m x L 0.80 m) and a 0.760 mm Sweco screen. The initial charge settings for the mill circuit were derived from previous lab work conducted on the Storforshei iron ores (Sandvik et al., 2012). The initial charge was set to 250 kg, and the mill was run at 36 rpm (i.e., 71.3 % of critical speed). During operation, the mill was fed with a series of discrete solid batches and a continuous addition of water corresponding to a pulp thickness of 60 wt % solids. The feed rate was manually adjusted to obtain a stable mill charge. For Kvannevann, torque, power, mill charge, and water feed rate were recorded automatically every second, whereas manual logging at 2-minute intervals was used when processing the Stensundtjern and Stortjønna samples. The mill feed and the mill circuit product were sampled for all three deposits.

4 Results

4.1 Ore types and mineral textures

4.1.1 Granular-Hematite

The Granular-Hematite ore type demonstrates a sugar-grained hematite texture, supported by more competent mm-sized quartz layers (Figure 2a). By measuring the longest axis in thin sections, the estimated average grain size of hematite was 200 µm. Granular-Hematite is characterised on the microscale by a random orientation of hematite grains within in the layers. The hematite is equigranular, with tabular shape, and has straight grain boundaries. Disseminated hematite grains (≈ 10 µm) occur in the quartz-rich layers. Some grains of carbonate minerals are present (Figure 3a).

4.1.2 Specular-Hematite

Deer et al. (1992) define specular hematite or specularite as "crystalline material with metallic lustre." Specular-Hematite has a characteristic flaky appearance in hand specimen (Figure 2b), and is frequently banded, with alternating mm-sized layers of quartz or carbonates and hematite. The layers are usually folded (Figure 3b). Under the microscope, Specular-Hematite is similar to the Granular-Hematite, demonstrating equigranular textures and straight grain boundaries. However, Specular-Hematite is distinguished by the overall grain size, averaging between 400-500 µm. Hematite grains are tabular, elongated, and oriented parallel to the layering (Figure 3b).

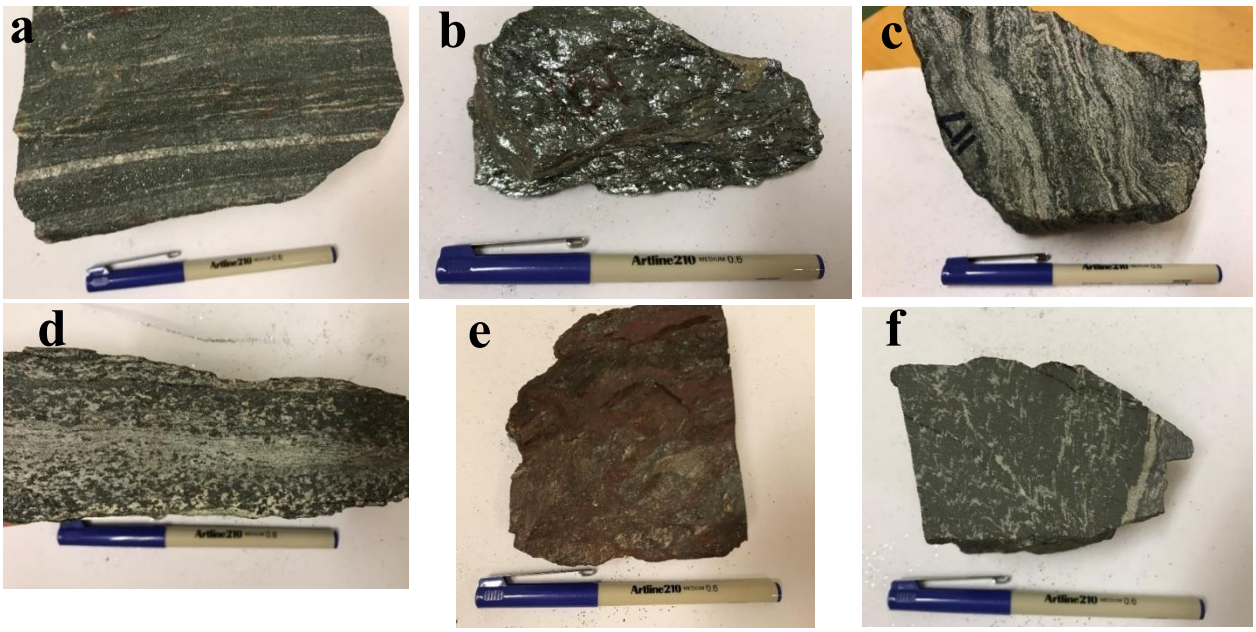

Figure 2: (a) Granular-Hematite, (b) Specular-Hematite, (c) Hematite-Magnetite, (d) Magnetite-Ore, (e) Mylonitic-Hematite, and (f) Massive-Hematite. (The scale is 13.5 cm)

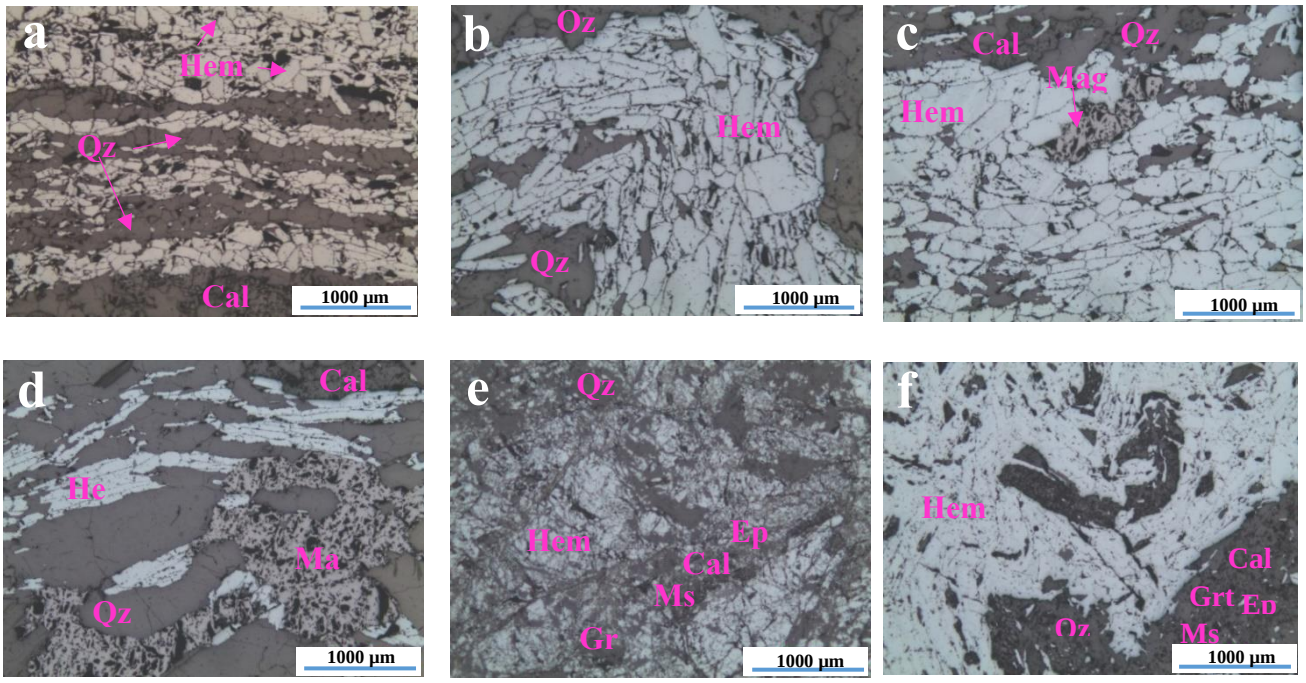

Figure 3: Reflected light photomicrographs showing typical hematite texture for the different ore types. (a) Granular-Hematite, (b) Specular-Hematite, (c) Hematite-Magnetite, (d) Magnetite-Ore, (e) Mylonitic-Hematite, and (f) Massive-Hematite. Mineral abbreviations after Whitney et al. (2010).

4.1.3 Hematite-Magnetite

The Hematite-Magnetite ore type is dominated by hematite and shows magnetite content typically in the range of 1-2 % in Kvannevann and 9-10 % in specimens from Stensundtjern. The texture of the

hematite in hand specimens varies between sugar-grained and flaky. It can also be banded, with quartz and/or calcite layers in-between hematite/magnetite layers (Figure 2c) and is typically folded similarly to the Specular-Hematite. The average hematite grain size is 300 µm with typical shape preferred orientation (SPO), whereas the grain size of magnetite is typically 1 mm (Figure 3c), without any visible SPO. Grain boundaries are straight within the hematite layers, and towards the quartz-calcite layers. Magnetite grain boundaries are typically irregular. The grain shape of iron oxides differs, with the magnetite having an equant-irregular shape, while the hematite is tabular (Figure 3c).

4.1.4 Magnetite-Ore

The Magnetite-Ore type is coarse-grained (average grain size 0.5 cm) (Figures 2d and 3d), and consists mainly of magnetite, with minor quartz, calcite, and small amounts of hematite (< 3 %). The magnetite grains are typically equant to irregular, while the hematite is tabular. The grain boundaries are straight to irregular.

4.1.5 Mylonitic-Hematite

Mylonitic-Hematite is, in hand specimen, characterised by a distinct red colour (Figure 2e). Hematite, quartz, and calcite grains (10-20 µm) are disseminated in a fine-grained matrix of gangue minerals, where individual minerals are difficult to distinguish. However, quartz, hematite, calcite, epidote, mica, and garnet were identified by SEM-EDS analyses. Some remnants of hematite grains (200-500 µm) can be found, with cracks filled with fine-grained recrystallised hematite, and gangue minerals (Figure 3e). The few observed grain boundaries are irregular. The term Mylonitic-Hematite refers to the presence of textures related to tectonic activity.

4.1.6 Massive-Hematite

The Massive-Hematite ore type is a fine-grained hematite ore, with massive hematite and irregularly folded layers or veins of fine-grained gangue (Figure 2f). Individual hematite grains are not easily distinguished, but grain boundaries appear to be irregular (Figure 3f). SEM-EDS show that the gangue consists mainly of quartz, calcite, garnet, epidote, and mica.

4.2 Distribution of lithologies

The lithologies defining the Storforshei IF iron ores were previously established during drill core logging by RG AS. For the present study, the lithologies were re-defined to comprise the six ore types defined in this paper and hence, improve the link between ore lithology and grindability. However, by using the original lithology descriptions, some correlations can be made (Table 1).

Table 1: Lithologies logged by RG AS, and their possible corresponding ore types.

Lithologies logged by RG AS	Ore types

Hematite ore (grained or specular annotation are often used in the comments)	Granular-Hematite, Specular-Hematite, can also include Massive-Hematite and Mylonitic-Hematite
Magnetite-hematite ore	Hematite-Magnetite
Magnetite ore	Magnetite-Ore
Hematite mylonite	Mylonitic-Hematite

Figure 4 shows the relative distribution of the original ore lithologies, as well as the most important host rocks in the three deposits. The relative distribution is based on the length of intersection in drill holes. Ore lithologies that could not be linked to a specific ore type were combined in one group (Other). The Kvannevann data in Figure 4 represents a larger area (Ørtfjellet) and contain data from some small ore deposits in addition to the Kvannevann deposit. Small variations are known in the ores of the Ørtfjellet area, but to the best knowledge of the authors, Figure 4 is a good representation of the lithologies observed in the Kvannevann deposit.

The most frequent ore type in Kvannevann is the Hematite ore, followed by the group "Other". Additionally, Kvannevann contains significant amounts of magnetite ore with minor magnetite-hematite ore. Stortjønna also contains magnetite ore. The hematite mylonite is found in minor content in Stortjønna, however, based on recent field observations it also occurs in the Ørtfjellet area. Stensundtjern contains hematite ore but is dominated by magnetite-hematite ore and has significant amounts of magnetite ore. The main host rocks are calcareous mica schist, mica schist, and marbles. Mylonite is predominantly found in Stortjønna but occur in all three deposits. Mylonite is used as a collective term for very fine-grained rocks that are found in veins at the ore-host rock contact. They are dominated by garnet, with varying contents of quartz, manganocalcite, and epidote.

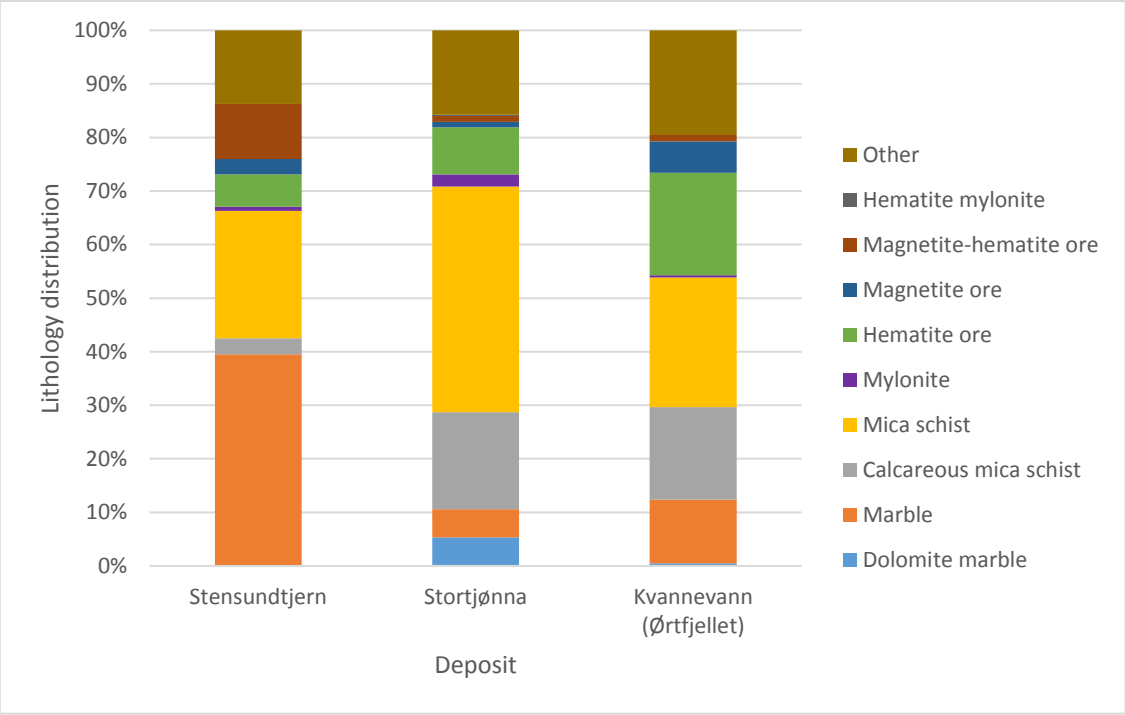

Figure 4: Lithological composition of the three deposits.

4.3 Surface hardness results

Minitab®17 (Minitab Inc., 2017) was used to prepare and analyse cumulative distribution plots for the surface hardness data. The data have been examined graphically and summary statistics calculated to identify differences between deposits and ore types. Schmidt hammer and Equotip measurements were not conducted on the same specimen; hence, they cannot be plotted in a scatter plot to investigate correlations. The results can, however, be used to compare the surface hardness of the different ore types.

4.3.1 Surface hardness by Schmidt hammer

Summary statistics from the Schmidt hammer measurements by Schmidt hammer of samples from Kvannevann, Stensundtjern, and Stortjønna are listed in Table 2. The lowest average surface hardness measured are in Specular-Hematite from Kvannevann and Stensundtjern, and Granular-Hematite from Kvannevann. Mylonitic-Hematite in Stortjønna has the highest surface hardness measured by Schmidt hammer. The surface hardness values in Kvannevann have a higher range than the surface hardness values in Stensundtjern, which is also reflected in the lower standard deviation in the surface hardness values in Stensundtjern. The maximum values for Massive-Hematite and Mylonitic-Hematite in Stortjønna are higher than the maximum values for Granular-Hematite and Specular-Hematite in Kvannevann and Stensundtjern, while the minima are similar for the four ore types.

Table 2: Summary statistics of Schmidt hammer measurements of Kvannevann, Stensundtjern, and Stortjønna. n.a. = not available.

Schmidt hammer measurement (N/mm^2)				
	Granular-Hematite	Specular-Hematite	Mylonitic-Hematite	Massive-Hematite
Mean				
Kvannevann	38	33	n.a.	n.a.
Stensundtjern	47	35	n.a.	n.a.
Stortjønna	n.a.	n.a.	52	45
Standard deviation				
Kvannevann	8.4	8.1	n.a.	n.a.
Stensundtjern	4.7	4.9	n.a.	n.a.
Stortjønna	n.a.	n.a.	9.9	8
Max				
Kvannevann	56	52	n.a.	n.a.
Stensundtjern	56	47	n.a.	n.a.
Stortjønna	n.a.	n.a.	75	65
Min				
Kvannevann	22	17	n.a.	n.a.
Stensundtjern	38	27	n.a.	n.a.
Stortjønna	n.a.	n.a.	34	29
Number of observations				
Kvannevann	160	260	n.a.	n.a.
Stensundtjern	40	60	n.a.	n.a.
Stortjønna	n.a.	n.a.	60	80

The differences in surface hardness values by Schmidt hammer are illustrated with cumulative distribution plots (Figure 5). An apparent difference in surface hardness can be seen, with Stortjønna having a mean of 48 N/mm^2, Stensundtjern with a mean value of 40 N/mm^2, and Kvannevann with a mean value of 35 N/mm^2.

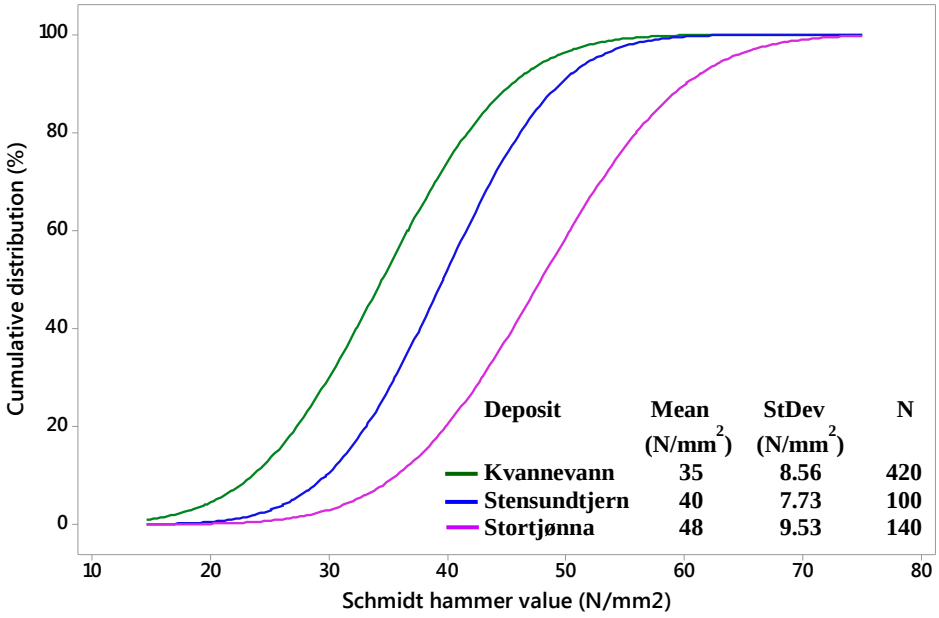

Figure 5: Cumulative distribution of surface hardness values by Schmidt hammer for each deposit irrespective of ore type.

Figure 6 illustrates surface hardness for the different ore types. Mylonitic-Hematite shows the highest surface hardness values, with P_{80} at 60 N/mm^2, while Massive-Hematite samples from Stortjønna and Granular-Hematite from Stensundtjern have the second highest values, with P_{80} at 52 N/mm^2 and 51 N/mm^2, respectively. For Kvannevann Granular-Hematite P_{80} is 44 N/mm^2. Specular-Hematite from Kvannevann and Stensundtjern have the lowest surface hardness values by Schmidt hammer with a P_{80} at 38 N/mm^2 and 39 N/mm^2, respectively.

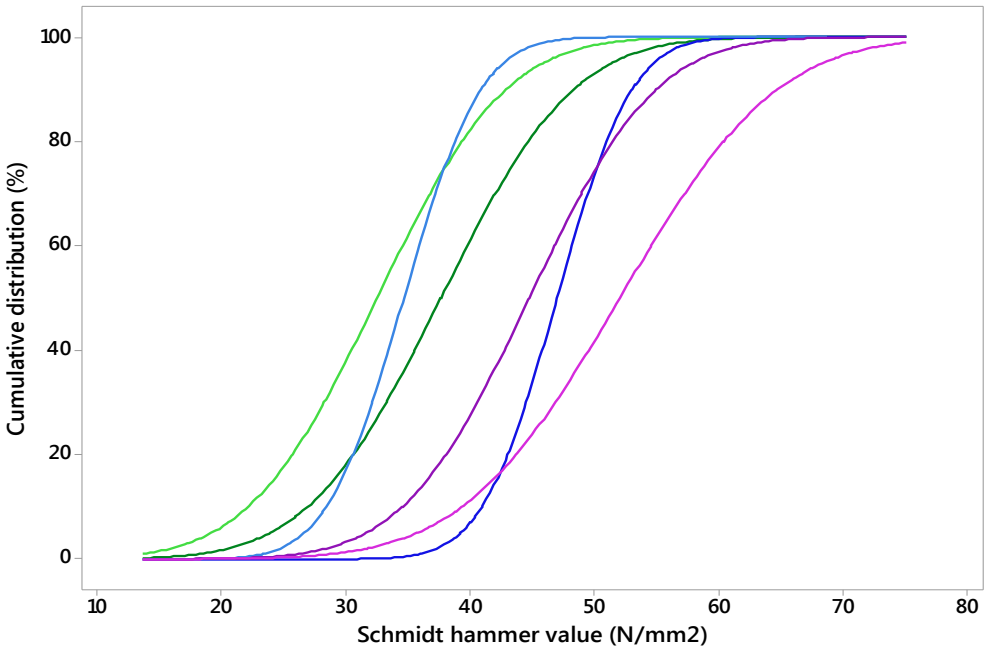

Deposit	Ore type	Mean (N/mm^2)	StDev (N/mm^2)	N
Kvannevann	Granular-Hematite	38	8.35	160
Kvannevann	Specular-Hematite	33	8.10	260
Stensundtjern	Granular-Hematite	47	4.72	40
Stensundtjern	Specular-Hematite	35	4.86	60
Stortjønna	Massive-Hematite	45	7.97	80
Stortjønna	Mylonitic-Hematite	52	9.91	60

Figure 6: Cumulative distribution of surface hardness values by Schmidt hammer in the ore types in the three deposits.

In Figure 7, the surface hardness values by Schmidt hammer are displayed according to ore types, the presence or absence of foliation, and the measurement direction. Most of the ore types are banded, and measurements have been collected both parallel and perpendicular to the foliation (LF and PF respectively). Some samples of Mylonitic-Hematite showed no foliation (NF). Surface hardness of Granular-Hematite and Specular-Hematite show a deposit-dependent variation and have highest values both for LF and PF in Stensundtjern. For Mylonitic-Hematite, PF-values are higher (P_{80} of 66 N/mm^2) than the LF-values (P_{80} of 53 N/mm^2). For Mylonitic-Hematite (NF) have a P_{80} of 57 N/mm^2 (Figure 7).

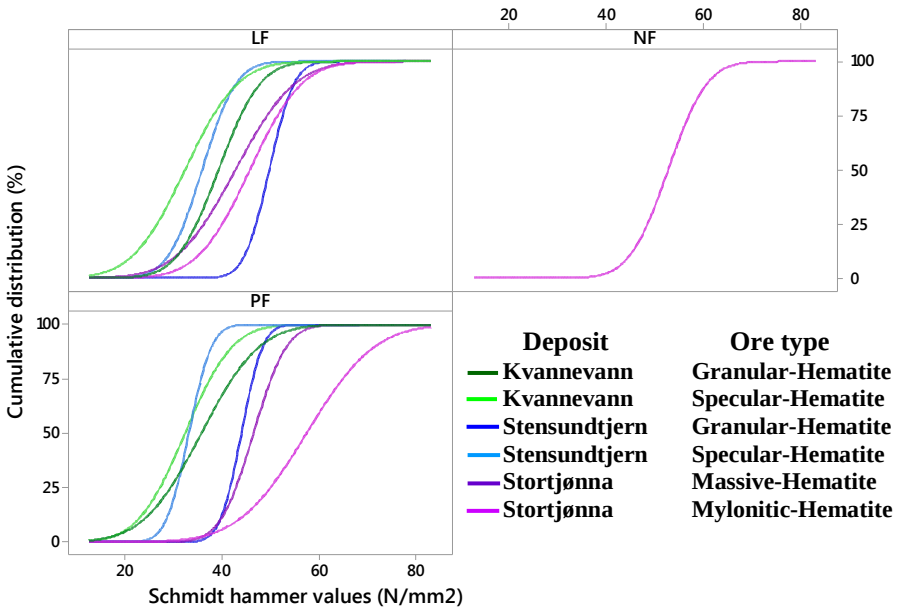

Figure 7: The cumulative distribution of surface hardness by Schmidt hammer for the ore types, divided into measurements collected perpendicular to the foliation (PF), parallel to the foliation (LF) and without any foliation (NF).

4.3.2 Surface hardness by Equotip

Summary statistics for Equotip measurements according to ore types and deposits are reported in Table 3. Mylonitic-Hematite in Stortjønna returned the highest average surface hardness (711 HLD), while Granular-Hematite and Specular-Hematite in Kvannevann returned the lowest surface hardness (533 HLD and 575 HLD respectively). The maximum and minimum surface hardness values appear to be random for all ore types in the three deposits. The maximum surface hardness values for ore types in Stortjønna are at the higher end of the scale, while all ore types in Kvannevann have minimum surface hardness under 200 HLD. The standard deviation is high for all ore types in the three deposits, especially for Granular-Hematite, Mylonitic-Hematite, and Massive-Hematite in Stortjønna. Mylonitic-Hematite and Massive-Hematite were not found in the core logs from Kvannevann and Stensundtjern.

Table 3: Summary statistics for the Equotip measurements divided into ore types and deposits. n.a. = not available.

Equotip measurements (HLD)						
	Granular-Hematite	Specular-Hematite	Hematite-Magnetite	Magnetite-Ore	Mylonitic-Hematite	Massive-Hematite
Mean						
Kvannevann	533	575	619	668	n.a.	n.a.
Stensundtjern	651	595	645	649	n.a.	n.a.
Stortjønna	649	626	633	669	711	648

Standard deviation						
Kvannevann	115.4	118	110.4	110.3	n.a.	n.a.
Stensundtjern	115.2	114.5	103.2	122.8	n.a.	n.a.
Stortjønna	133.8	121.2	113.9	104.3	136.5	137.7
Max						
Kvannevann	832	878	807	874	n.a.	n.a.
Stensundtjern	844	834	814	860	n.a.	n.a.
Stortjønna	865	852	875	864	896	864
Min						
Kvannevann	106	128	129	195	n.a.	n.a.
Stensundtjern	236	250	363	155	n.a.	n.a.
Stortjønna	167	154	183	251	378	126
Number of observations						
Kvannevann	1153	1852	390	195	n.a.	n.a.
Stensundtjern	697	471	269	286	n.a.	n.a.
Stortjønna	237	90	58	120	39	440

Figure 8 shows the cumulative distribution of surface hardness values using Equotip for all deposits. Stortjønna has the highest values, with a P_{80} of 762 HLD, followed by Stensundtjern and Kvannevann, with P_{80} of 731 HLD and 672 HLD, respectively. The average surface hardness in Stortjønna is 650 HLD, whereas 635 HLD in Stensundtjern, and 571 HLD for Kvannevann. The number of measurements (N) in each deposit varies (Figure 8).

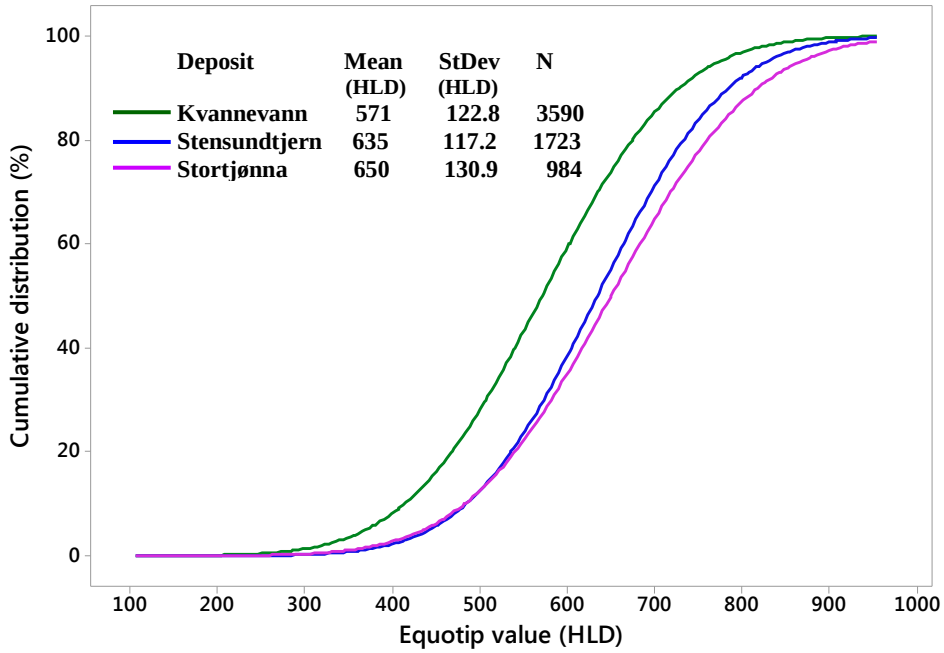

Figure 8: Cumulative distribution of surface hardness values using Equotip in Kvannevann, Stensundtjern, and Stortjønna.

The surface hardness values by Equotip for the ore types and their cumulative distribution are shown in Figure 9. Average surface hardness varies between 711 HLD for Mylonitic-Hematite and 576 HLD for Specular-Hematite.

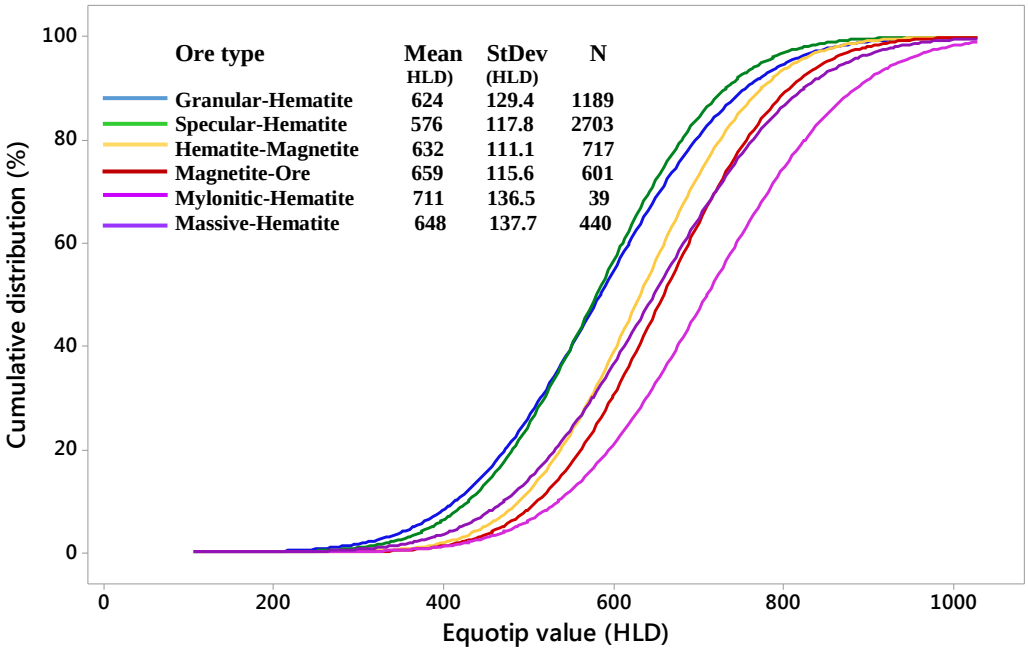

Figure 9: The cumulative distribution of surface hardness values by Equotip for the ore types regardless of the deposits.

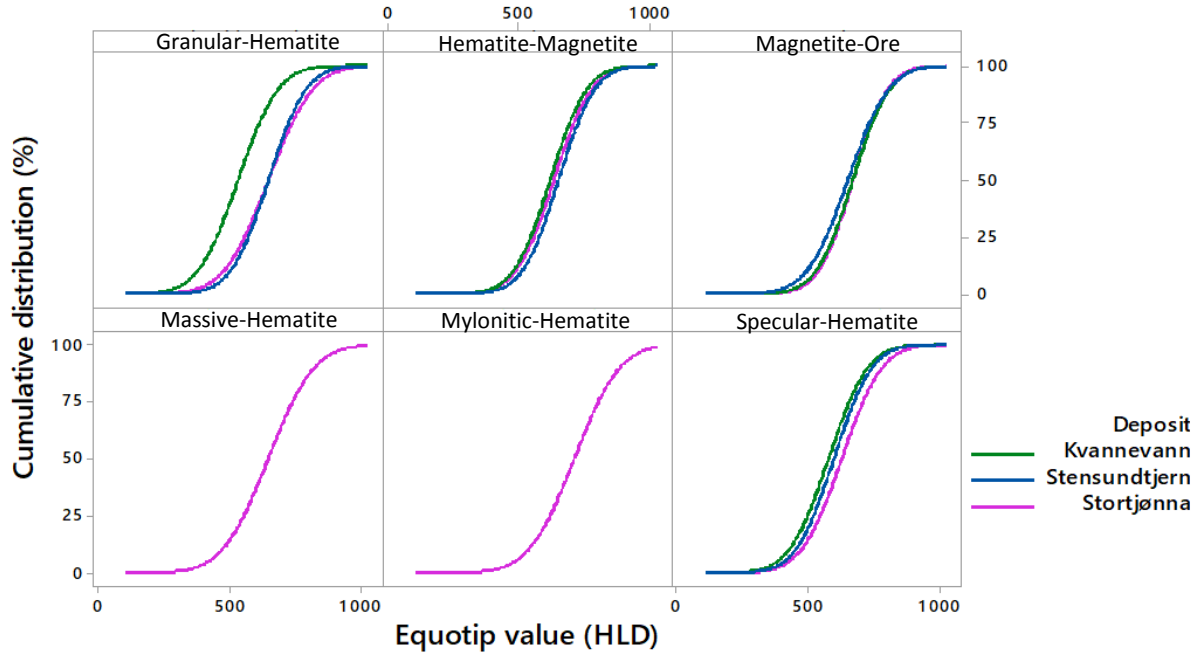

Figure 10: Surface hardness values using Equotip for ore types in the three deposits.

The surface hardness measurements of the ore types in the three deposits using the Equotip are compared in Figure 10. Specular-Hematite, Hematite-Magnetite, and Magnetite-Ore types display similar surface hardness values by Equotip in the three deposits. The Granular-Hematite from Kvannevann have lower surface hardness by Equotip than Granular-Hematite from Stensundtjern and Stortjønna. This is also apparent from Table 3.

4.4 Pilot-scale AG milling

To obtain a stable circuit, the solid feed rate had to be adjusted for each ore type. The final steady-state solid feed rates, the resulting mill torque, and specific energy consumption are summarised in Table 4. Figs. 11-13 show the data recorded during the experiments.

Table 4: Solid feed rate, mill torque, and mill power during steady-state milling of the Kvannevann, Stensundtjern, and Stortjønna ores.

	Time (hh:mm)	Solid feed rate (kg/h)	Mill torque (kN)	Mill power (kW)
Kvannevann	01.30-03.00	266	530.5	2.2

Stensundtjern	01:00-03:00	150	367.5	1.6
Stortjønna	02:30-04:30	100	522.6	2.2

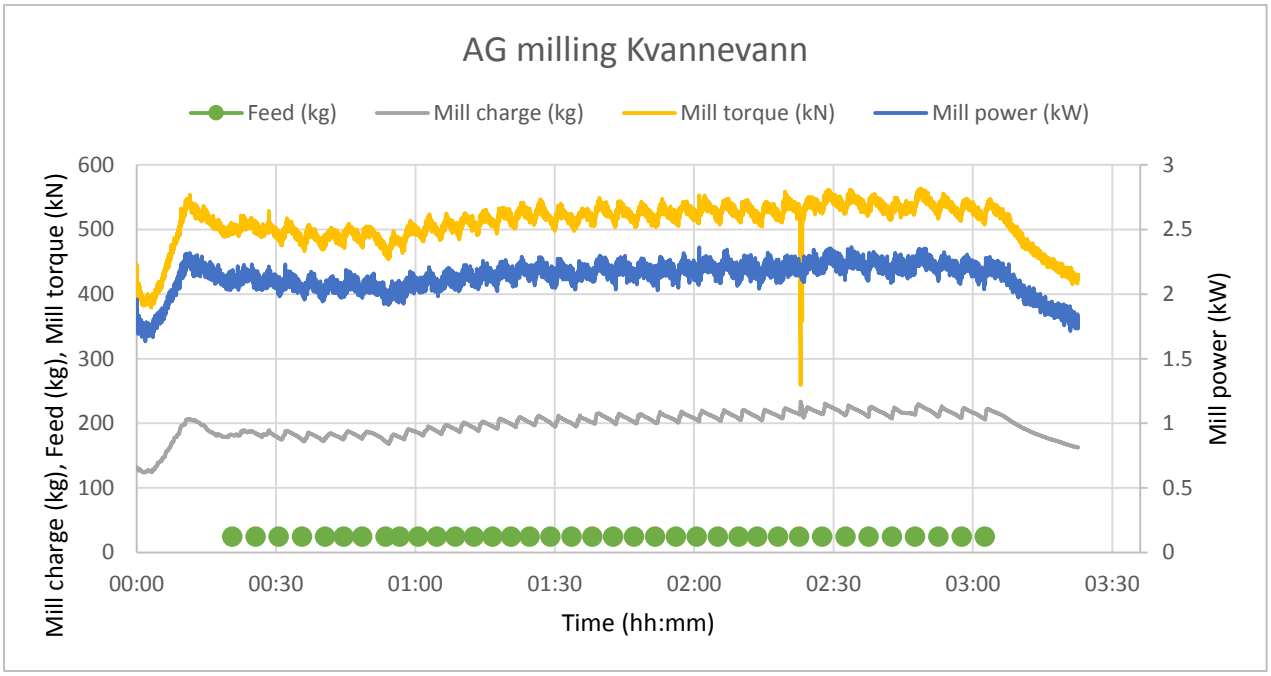

Figure 11: Kvannevann milling results.

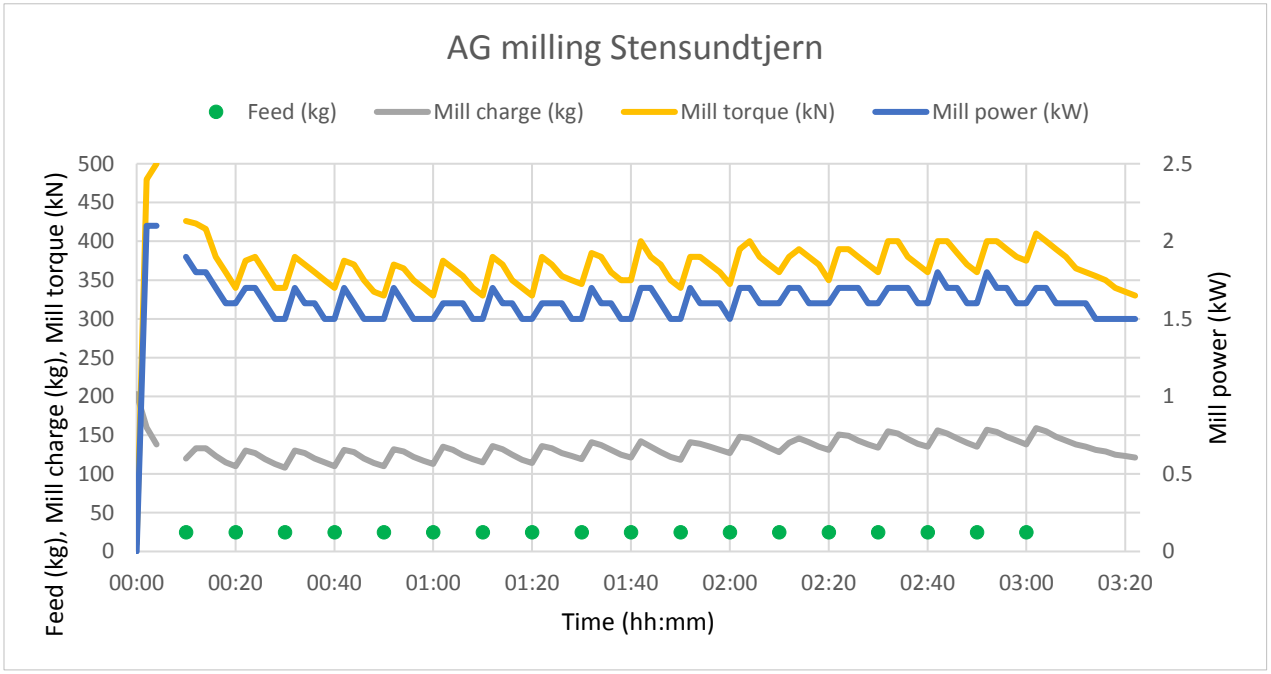

Figure 12: Stensundtjern milling results.

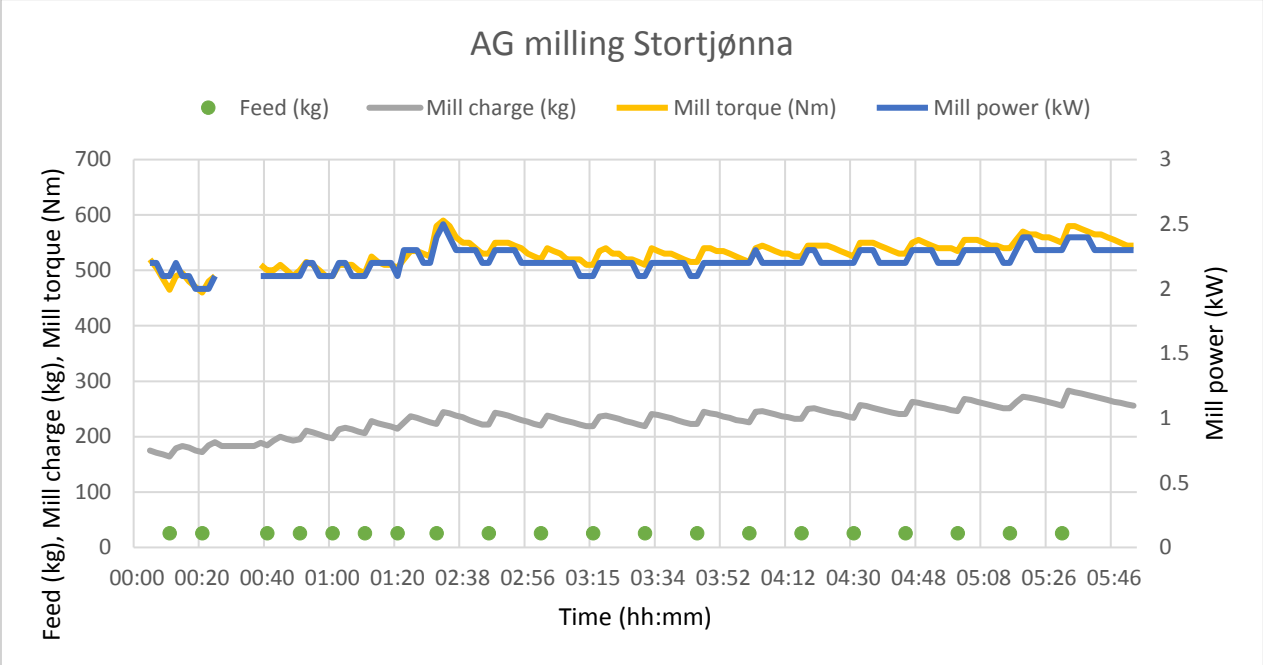

Figure 13: Stortjønna milling results.

4.5 Particle size distribution

Samples collected from both the mill feed and the mill product were sieved on a rot-tap sieve shaker using the W.S. Tyler sieves series. Figure 14 presents the particle size distribution (PSD) for the mill feed of all three deposit samples. The d_{50} values were found to be 70 mm, 38 mm, and 100 mm for Kvannevann, Stensundtjern, and Stortjønna, respectively.

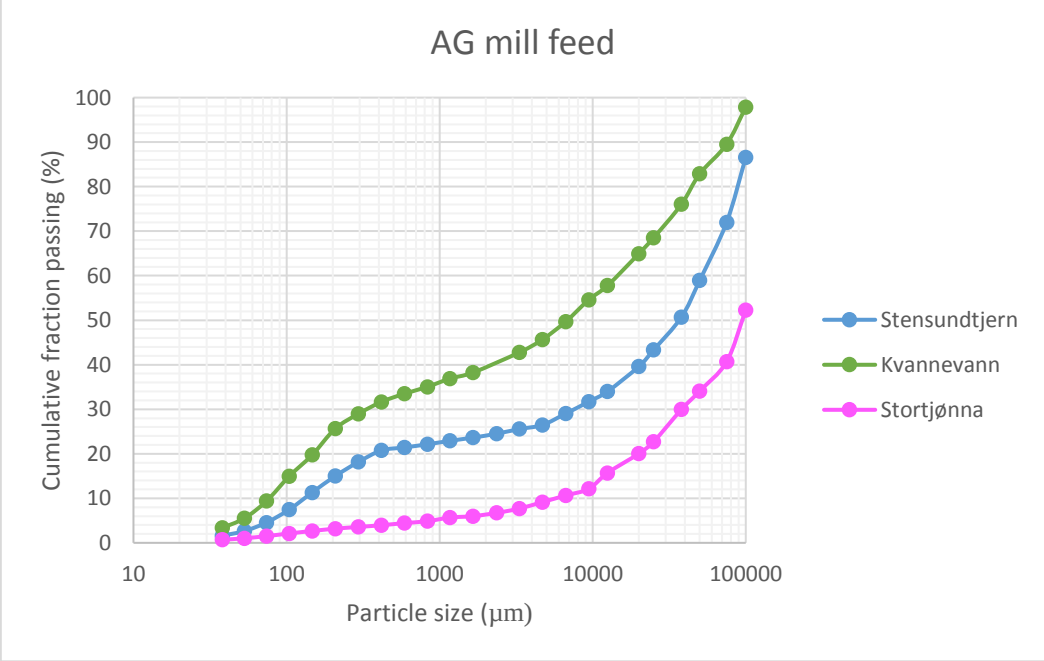

Figure 14: Particle size distribution of the mill feed.

Figure 15 shows the particle size distribution of the mill circuit products from Kvannevann, Stensundtjern, and Stortjønna. The Stortjønna mill circuit product has a $d_{80} \approx 147$ µm and is thus the finest product. The Kvannevann mill circuit product also has relatively fine material with $d_{80} \approx 170$ µm. The Stensundtjern mill circuit product shows a coarser particle size distribution compared with the other two with $d_{80} \approx 280$ µm. Stortjønna contains substantial amounts of fines (< 38 µm) compared to Kvannevann and Stensundtjern.

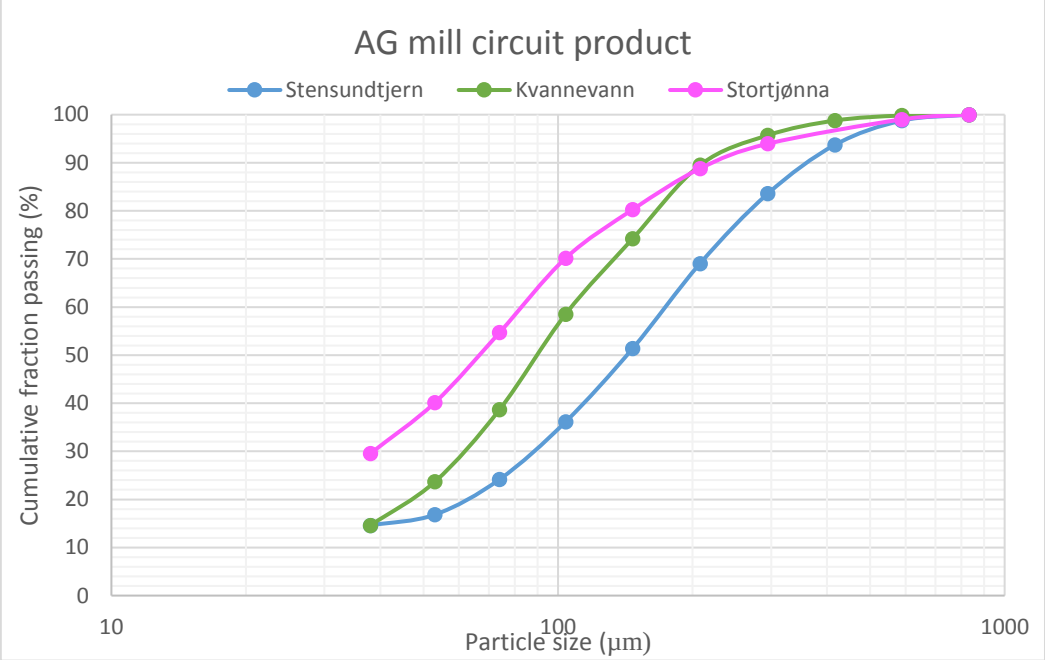

Figure 15: The particle size distributions of Kvannevann, Stensundtjern, and Stortjønna mill circuit products.

5 Discussion

5.1 The relationship between ore mineralogy, texture, and surface hardness

The defined ore types show significant differences in mineral textures. The most pronounced characteristics can be summarised as:

Granular-Hematite and Specular-Hematite are mainly similar, although some differences in hematite grain shapes are seen in hand specimen (Figure 2). Hematite is mostly banded and relatively coarse-grained (200-500 µm), with small hematite grains (≈ 10 µm) disseminated in bands dominated by quartz or carbonates.

Hematite-Magnetite and Magnetite-Ore have a coarse-grained texture, especially the magnetite grains, which range from 1-5 mm (Figure 3 c and d) (the coarsest magnetite is found in Magnetite-Ore). Hematite and magnetite have straight and irregular grain boundaries, respectively.

Hematite-Magnetite and Magnetite-Ore are mainly distinguished by the high hematite content in Hematite-Magnetite.

Mylonitic-Hematite typically contains fine-grained hematite, disseminated in a fine-grained matrix of gangue minerals. There are also relics of coarse-grained hematite in the matrix.

Massive-Hematite is dominated by fine-grained hematite, without clearly distinguishable grain boundaries, with veins consisting of a matrix of fine-grained minerals, mainly quartz, mica, feldspar, epidote, and garnet.

Quantified by the Equotip, the Granular-Hematite in Kvannevann exhibits lower surface hardness values than Granular-Hematite in Stensundtjern and Stortjønna (Figure 10). While exhibiting similar textures, varying amounts of gangue affect the surface hardness. The increased surface hardness is caused by a high quartz content in Granular-Hematite. Hence, the ore type can be divided into two subgroups: high-quartz Granular-Hematite found in Stensundtjern and Stortjønna, and low-quartz Granular-Hematite found in Kvannevann. The slightly lower surface hardness of Specular-Hematite compared with Granular-Hematite is related to the flaky hematite textures in Specular-Hematite, resulting in less competent hematite bands. Table 5 shows surface hardness measurements by Equotip and important textural properties of the six ore types.

Table 5: Surface hardness by Equotip and textural properties of ore minerals in the six ore types.

Ore type	Average surface hardness by Equotip (HLD)	Average grain size	Grain shape	Grain boundaries
Granular-Hematite	624	hematite: 200 µm	hematite: tabular	Straight
Specular-Hematite	576	hematite: 400-500 µm	hematite: tabular	Straight
Hematite-Magnetite	632	hematite: 300 µm magnetite: 1 mm	hematite: tabular magnetite: equant-irregular	Straight to irregular
Magnetite-Ore	659	magnetite: 0.5 cm	magnetite: equant-irregular hematite: tabular	Straight to irregular
Mylonitic-Hematite	711	Disseminated hematite: 10-20 µm	hematite: irregular	Irregular to not visible

Massive-Hematite	648	Single grains are difficult to identify	Grain shapes are difficult to identify	Boundary between massive hematite and gangue: irregular

The Hematite-Magnetite and Magnetite-Ore have higher surface hardness values by Equotip than Granular-Hematite and Specular-Hematite, although all four have approximately the same hematite grain sizes. Possible explanations for high values are irregular grain boundaries of the equant-irregular magnetite grains, or the higher contents of magnetite in the Hematite-Magnetite and the Magnetite-Ore. The high surface hardness by Equotip in Mylonitic-Hematite and Massive-Hematite can be explained by the fine-grained texture, and irregular to no visible grain boundaries. Based on the ore mineralogy, textures, and surface hardness values presented in the results, the ore types can be divided into three groups (Table 6).

Table 6: Ore types divided into three groups based on surface hardness measurements.

Surface hardness group	Ore type
Low hardness	Granular-Hematite and Specular-Hematite
Intermediate hardness	Hematite-Magnetite and Magnetite-Ore
High hardness	Mylonitic-Hematite and Massive-Hematite

The surface hardness measurements by Schmidt hammer confirm the same trend as the surface hardness values by Equotip, with the lowest surface hardness values obtained for Specular-Hematite and Granular-Hematite whereas Mylonitic-Hematite and Massive-Hematite have the highest surface hardness (Table 2). The standard deviation of the surface hardness values by Schmidt hammer in Stensundtjern is lower than for the same ore types in Kvannevann, indicating more homogeneous ore types in Stensundtjern (Table 2). The measurement direction relative to foliation has only a minor effect on surface hardness for the banded ore types Granular-Hematite, Specular-Hematite, and Massive-Hematite (Figure 7). Due to lack of suitable specimens for surface hardness measurements, Hematite-Magnetite and Magnetite-Ore have not been tested with the Schmidt hammer and the total number of specimens tested was limited. Hence, the following discussion will focus on the surface hardness values by Equotip.

5.2 The effect of ore mineralogy and textures on grindability

Unlike Mwanga et al. (2015) who focused on mill tests on small (220 g) relatively homogeneous ore types or units, the mill testing presented in this paper was carried out on a larger scale (1-2 tonnes) to represent the mineralogical and textural variability between the three deposits. Xu et al. (2013) postulated that ore with straight grain boundaries and coarse grains will break more easily, and that low specific energy is sufficient for grain boundary fractures to occur. This agrees with the results of the present study. The Kvannevann sample, dominated by coarse-grained hematite, required a solid feed rate of 266 kg/h for the mill to reach steady state (Figure 11). This is almost three times the corresponding rate for the Stortjønna sample, dominated by fine-grained hematite, where the solid feed rate was 100 kg/h. Mill power and torque were approximately the same for the Stortjønna- and the Kvannevann sample, indicating lower grindability for the Stortjønna sample given the lower solid feed rate. The Stensundtjern sample achieved steady-state with a solid feed rate of 150 kg/h. Hence, the grindability was lower than for the Kvannevann sample. This is probably partly related to a finer-grained mill feed for the Kvannevann sample than the Stensundtjern sample (Figure 14), making the Kvannevann sample easier to grind. Another factor affecting the grindability is the relatively high content of Hematite-Magnetite at Stensundtjern, where the magnetite has irregular grain boundaries.

The Stortjønna mill feed was coarser than the Kvannevann- and Stensundtjern mill feeds, while the mill circuit product was finer-grained compared to the corresponding samples from Kvannevann and Stensundtjern. A coarse feed also suggests a lower grindability in Stortjønna, with a longer residence time in the mill, creating a fine-grained mill circuit product. Stensundtjern has an intermediate feed size but produces the coarsest mill circuit product. The mill tests compared to mineralogical and textural characteristics indicate that grain size and shape, combined with the structure of grain boundaries, influence grindability. These results confirm the work by Kekec et al. (2006), Mwanga et al. (2015), and Xu et al. (2013).

5.3 Using surface hardness to evaluate grindability

The weighted average surface hardness by Equotip was calculated from the distribution of lithologies in the deposits (Figure 4). Based on geological mapping, the ore logged as Hematite ore in Stensundtjern and Kvannevann was assumed to consist of Granular-Hematite and Specular-Hematite, while Hematite ore in Stortjønna was assumed to consist of Mylonitic-Hematite and Massive-Hematite. Thus, the surface hardness of the ore types can be related to the performance in the mill tests. Table 7 shows the relationship between arithmetic- and weighted average surface hardness by Equotip (HLD), arithmetic average surface hardness by Schmidt hammer (N/mm^2), throughput, and specific energy consumption during milling in the three deposits.

Table 7: Relationship between average surface hardness, throughput, and specific energy consumption during steady state milling for the three deposits.

	Surface hardness			Mill performance	
Deposits	Weighted average (HLD)	Arithmetic average (HLD)	Arithmetic average (N/mm^2)	Throughput (kg/h)	Specific energy consumption (kWh/tonne)
Kvannevann	574	571	35	266	8.27
Stensundtjern	640	635	40	150	10.7
Stortjønna	674	650	48	100	22.0

Kvannevann has the lowest surface hardness values, high throughput, and relatively low specific energy consumption, indicating high grindability. Stortjønna has the highest surface hardness, low throughput, and substantially higher specific energy consumption, indicating low grindability. Stensundtjern has intermediate surface hardness, a lower throughput, and slightly higher specific energy consumption than Kvannevann, hence, intermediate grindability. This suggests that it should be possible to use simple surface hardness measurements to evaluate grindability. The available sample material will determine whether Equotip or Schmidt hammer is the best surface hardness method in a mining operation. Equotip cannot be used on irregular surfaces and hence, is best suited for use on drill cores. The Schmidt hammer, on the other hand, is better suited for large-sized boulders. For statistical and efficiency reasons the Equotip is the preferred method, and drill cores are often readily available on most mine sites.

6 Conclusion

The presented research shows that the grindability of the different ores is affected by ore mineralogy and texture in addition to Fe grade. This corresponds well with on-site experiences. The six ore types defined can be placed into three groups based on their surface hardness values (Table 6).

The main textural characteristics influencing surface hardness are grain size and grain boundaries, as fine-grained ore types with irregular-to-no visible grain boundaries show the highest surface hardness. Whether ore mineralogy (magnetite content) influences surface hardness is difficult to determine and needs further investigation. Ore types with coarse-grained iron oxides and straight grain boundaries have higher throughput and lower specific energy consumption, thus a higher grindability, than fine-grained ore types with irregular-to-no visible grain boundaries. The results of this research show how surface hardness measurements combined with characterisation of ore mineralogy and textures can be used to evaluate grindability. To further investigate the relationship between ore mineralogy and texture, and grindability, automated mineralogy should be performed on the mill circuit products. Such

results may also be used to predict the material's performance in the magnetic separation, which is the next step in the processing of this iron ore, and ultimately the recovery of iron. Identifying key ore characteristics, and knowledge of how they affect mineral processing can lead to better production control and utilisation of ore bodies. The choice of surface hardness measurement method strongly depends on the available sample material. In general surface hardness measurements on drill cores using the Equotip is more efficient than the measurements using Schmidt hammer on larger specimens and provides more results in a shorter time. The disadvantage with the Equotip is that a flat sample surface is required. However, as most mine sites have available drill cores from drill campaigns, drill core availability is rarely an issue.

7 Acknowledgements

This research is funded by the Research Council of Norway (project no. 232428) and RG AS through the industrial PhD scheme. Thanks also to senior geologist Alexander Kühn and geologist Marta Lindberg at RG AS for helping with sampling strategies and being good discussion partners. Thanks to workers in RG AS, Leonard Nilsen og Sønner (LNS), Heia Maskin and Øijord&Aanes AS for helping with the practical work concerning sampling; blasting, loading, transporting, crushing, and splitting. Finally, huge thanks to Helge Rushfeldt, Torkjell Breivik, and Kristin Bergseth Aure at IGB, NTNU for help with planning and running the pilot circuit.

8 References

Bond, F.C., 1952. The third theory of comminution. Transactions AIME Mining Engineering, 485 p.

Bugge J.A.W., 1948. Rana Gruber: Geologisk beskrivelse av jernmalmfeltene i Dunderlandsdalen. Norges Geologiske Undersøkelse No. 171.

Deer, W.A., Howie, R.A., and Zussman, J., 1992. An introduction to the rock forming minerals, 2nd edition. Pearson Education Limited, 685 p.

Deere, D.U., Miller, R. P., 1966. Engineering classification and index properties for intact rock. Technical report no. AFWL-TR-65-116, University of Illinois. 300 p.

Ellefmo, S., 2005. A probabilistic approach to the value chain of underground iron ore mining Doctoral thesis, NTNU. Trondheim, 205 p.

Gjelle, S., Søvegjarto, U., Tveiten, B., 1991. Dunderlandsdalen 2027 I, berggrunnsgeologisk kart 1: 50,000. Norges geologiske undersøkelse.

Grenne, T., Ihlen, P.M., Vokes, F.M., 1999. Scandinavian Caledonide Metallogeny in a plate tectonic perspective. Mineralium Deposita 34, pp. 422-471.

Hunt, J., Kojovic, T., and Berry, R., 2013. Estimating Comminution Indices from Ore Mineralogy, Chemistry and Drill Core Logging, The Second AUSIMM International Geometallurgy Conference, Brisbane, QLD.

International Society for Rock Mechanics, 1978. Commission on Standardization of Laboratory and Field Tests. Int. J. Rocks Mech. Min. Sci. & Geomech. Abstr. Vol. 15, pp. 89-97.

Kekec, B., Unal, M., and Sensogut, C., 2006. Effect of the textural properties of rocks on their crushing and grinding features. Journal of University of Science and Technology Beijing,) Mineral, Metallurgy, Material, 13(5), pp. 385-392.

Lopera, P.A.M., 2014. Geometallurgical mapping and mine modelling – comminution studies: La Colosa Case Study. *AMIRA P843A* Research Master Thesis. University of Tasmania, 75 p. (https://oatd.org/oatd/record?record=oai%5C%3Aeprints.utas.edu.au%5C%3A18741)

Lund, C., 2013. Mineralogical, chemical and textural characterisation of the Malmberget iron ore deposit for a geometallurgical model. Doctoral Thesis, LTU, Luleå, 190 p.

Melezhik, V.A., Ihlen, P.M., Kuznestov, A.B., Gjelle, S., Solli, A., Gorokhov, I.M., Fallick, A.E., Sandstad, J.S., Bjerkgård, T., 2015. Pre-Sturtian (800-730 Ma) depositional age of carbonates in sedimentary sequences hosting stratiform iron ores in the Uppermost Allochthon of the Norwegian Caledonides: A chemostratigraphic approach. Precambrian Research 261, pp. 272-299.

Minitab Inc., 2017. Minitab home page, Minitab Incorporated. Available from: http://www.minitab.com/en-us/ [11.09.2017]

Morrell, S., 2004. Predicting the specific energy of autogenous and semi-autogenous mills from small diameter drill core samples. Minerals Engineering 17, pp. 447-451.

Mwanga, A., Lamberg, P., Rosenkranz, J., 2015. Comminution test method using small drill core samples. Minerals Engineering 72, pp. 129-139.

Napier-Munn, T.J., Morrell, S., Morrison, R.D., Kojovic, T., 1996. Mineral Comminution Circuits: Their Operation and Optimalisation. Julius Kruttschnitt Mineral Research Centre, Australia.

NGU, 2017. Transcript from database Norwegian ores. http://geo.ngu.no/kart/mineralressurser_mobil/ [12.03.2018]

Niiranen, K., 2015. Characterization of the Kiirunavaara iron ore deposit for mineral processing with a focus on the high silica ore type B2. Diss., Leoben, Montanuniversität, Lehrstuhl für Aufbereitung und Veredlung.

Philander, C., Rozendaal, A., 2011. The contributions of geometallurgy to the recovery of lithified heavy mineral resources at the Namakwa Sands mine, West Coast of South Africa. Minerals Engineering 24, pp. 1357-1364.

Proseq, 2016. Operating instructions, Original Schmidt. Avaliable from: http://www.proceq.com/en/site/downloads/Original%20Schmidt.html [02.11.2016]

Operating instructions Equotip 3. Available from: http://www.proceq.com/site/downloads/Equotip%203.html [03.11.2016]

Roberts, D. and Gee, D.G., 1985. An introduction to the structure of the Scandinavian Caledonides. In: Gee, D.G., Sturt, B.A. (Eds.), The Caledonide Orogen – Scandinavia and Related Areas. John Wiley & Sons, Chichester, pp. 55–68.

Sandvik, K.L., Rein, A., Corneliussen, O., Kleiv, R.A., Larsen E., 2012. Autogenmaling av jernmalm fra Kvannevann og Stortjønna. M-RAK 2012:11, NTNU.

Shi, F., Kojovic, T., Larbi-Bram, S., Manlapig, E., 2009. Development of a rapid particle breakage characterisation device – the JKRBT. Minerals Engineering 22 (7-8), pp. 602-612.

Szilágyi, K., Borosnyói, A., 2009. 50 years of experience with the Schmidt rebound hammer. Concrete Structures 10, pp.46-56.

Søvegjarto, U., 1972. Berggrunnsgeologiske undersøkelser i Dunderlandsdalen, Nordland. Post graduate thesis. University of Oslo, 139p.

Søvegjarto, U., Marker, M., Graversen, O., Gjelle, S., 1989. Storforshei 2027 IV, berggrunnsgeologisk kart 1: 50,000. Norges geologiske undersøkelse.

Van Tonder, E., Deglon, D.A., Napier-Munn, T.J., 2010. The effect of ore blends on the mineral processing of platinum ores. Minerals Engineering 23 (8), pp. 621-626.

Viles, H., Goudie A., Grab, S., and Lalley J., 2011. The use of Schmidt hammer and Equotip for rock hardness assessment in geomorphology and heritage science: a comparative analysis. Earth Surface Processes and Landforms 36, pp. 320-333.

Voordouw, R.J., Gutzmer, J., and Beukes, N.J., 2010. Zoning of platinum group mineral assemblages in the UG2 chromitite determined through in situ SEM-EDS-based image analysis. Mineralium Deposita, 45(2), pp. 147-159.

Whitney, D.L. and Evans B.W., 2010. Abbreviations for names of rock-forming minerals. American Mineralogist, Vol. 95, pp. 185-187.

Xu, W., Dhawan, N., Lin, C-L., Miller, J.D., 2013. Further study of grain boundary fracture in the breakage of single multiphase particles using X-ray microtomography procedures. Minerals Engineering 46-47, pp. 89-94.